Changes in Imja Tsho in the Mt. Everest Region of Nepal

M. A. Somos-Valenzuela[1], D. C. McKinney[1], D. R. Rounce[1], and A. C. Byers[2],

[1] {Center for Research in Water Resources, University of Texas at Austin, Austin, Texas, USA}

[2] {The Mountain Institute, Washington DC, USA}

Correspondence to: D. McKinney (daene@aol.com)

Abstract

Imja Tsho, located in the Sagarmatha (Everest) National Park of Nepal, is one of the most studied and rapidly growing lakes in the Himalayan range. Compared with previous studies, the results of our sonar bathymetric survey conducted in September of 2012 suggest that its maximum depth has increased from 90.5 m to 116.3±5.2 m since 2002, and that its estimated volume has grown from 35.8±0.7 million m^3 to 61.7±3.7 million m^3. Most of the expansion of the lake in recent years has taken place in the glacier terminus-lake interface on the eastern end of the lake, with the glacier receding at about 52.1 m yr^{-1} and the lake expanding in area by 0.038 km^2 yr^{-1}. A ground penetrating radar survey of the Imja-Lhotse Shar glacier just behind the glacier terminus shows that the ice is over 200 m in the center of the glacier. The volume of water that could be released from the lake in the event of a breach in the damming moraine on the western end of the lake has increased to 34.1±1.08 million m^3 from 21 million m^3 estimated in 2002.

1   Introduction

The rate of formation of glacial lakes in the Nepal Himalaya has been increasing since the early 1960s (Bolch et al., 2008; Watanabe et al., 2009; Bajracharya and Mool, 2009). Twenty-four new glacial lakes have formed, and 34 major lakes in the Sagarmatha (Mt. Everest) and Makalu-Barun National Parks of Nepal have grown substantially during the past several decades (Bajracharya et al., 2007). Accompanying this increase in the number and size of glacial lakes is an associated increase in the risk of glacial lake outburst flood (GLOF) events (Ives et al., 2010; Shrestha and Aryal, 2011). At least twelve of the new or growing lakes within the Dudh

Koshi watershed of this region may be of concern, based on their rapid growth as evidenced by comparative time lapse, remotely sensed imagery over the past several decades (Bajracharya et al., 2007; Jianchu et al., 2007; Bolch et al., 2008; Watanabe et al., 2009).

GLOFs are the sudden release of a large amount of glacial lake water into a downstream watercourse, many orders of magnitude higher than the normal flow due to the of a moraine damming the lake (Carrivick and Rushmer, 2006). They can cause severe damage to downstream communities, infrastructure, agriculture, economic activities, and landscapes because of the sheer magnitude and power of the flood and debris flows produced (Bajracharya et al., 2007). The Khumbu region of Nepal (Figure 1) is often mentioned as an area prone to GLOF events. The appearance and possible danger posed by new glacial lakes in this region has prompted national and regional groups to begin assessing engineering and non-engineering methods to mitigate increasing GLOF risks to communities, infrastructure, and landscapes downstream of the lakes (e.g., UNDP, 2013).

Imja-Lhotse Shar glacier is located in the Imja Khola watershed in the Khumbu region (27.9^{o} N, 86.9^{o} E), about 9 km south of the summit of Mt. Everest. It is comprised of the Lhotse Shar glacier to the north and the Imja glacier to the east. The Amphu glacier appears to no longer contribute to the Imja-Lhotse Shar glacier. Bolch et al. (2011) studied the mass change for ten glaciers in the Khumbu region south and west of Mt. Everest, and found that the Imja-Lhotse Shar glacier exhibited the largest loss rate in the Khumbu region, -0.5 ± 0.09 m.w.e. yr^{-1} (meter water equivalent per year) for the period 1970-2007. Nuimura et al. (2012) also report significant surface lowering of the glaciers of this area, including -0.81 ± 0.22 m.w.e. yr^{-1} (1992-2008) and -0.93 ± 0.60 mw.e. yr^{-1} (2000–2008) for the Imja-Lhotse Shar glacier. Gardelle et al (2013) reported -0.70 ± 0.52 mw.e. yr^{-1} (1999–2011), Bolch et al. (2011) reported 1.45 ± 0.52 mw.e. yr^{-1} (2002–2007). The bathymetric survey reported here will help to refine the mass balance estimate of this glacier because it can be used to improve the quantification of the aqueous losses.

Hammond (1988), in one of the first studies in the region concerned with glacial lakes, identified twenty-four lakes and numerous other meltwater ponds in the Khumbu region in 1988. Most of these lakes began forming in the late 1950s to early 1960s, and have expanded considerably since then, especially the Imja Tsho (lake). For example, the 1963 Schneider map

1   of the Everest region does not show a lake on the Imja-Lhotse Shar glacier, but rather five small

2   meltwater ponds on the surface near the glacier's terminus (Hagen et al., 1963). The expansion

3   of Imja Tsho since the mid-1950s has been documented through the use of repeat oblique

4   photography (Byers, 2007) and remote sensing (Mool et al., 2001).

5   A number of authors have discussed the details of Imja Tsho's development (Quincey et

6   al., 2007; Bajracharya et al., 2007; Yamada, 1998; Watanabe et al., 2009; Ives et al., 2010;

7   Lamsal et al., 2011). Imja Tsho is bounded to the east by the Imja-Lhotse Shar glacier, to the

8   north and south by lateral moraines, and to the west by the moraine of the former glacier

9   terminus. The lateral moraine troughs act as gutters, trapping debris derived from rockfall, snow

10 avalanches, and fluvial transport (Hambrey et al., 2008). Imja Tsho is dammed by the 700 m

11 wide by 600 m long, ice-cored, debris-covered, former glacier tongue through which water exits

12 by means of an outlet lake complex (Watanabe et al., 1994, 1995). The former glacier tongue

13 still contains ice as clearly evidenced by outcrops of bare ice, ponds formed by melt water from

14 ice in the moraine, traces of old ponds (Yamada and Sharma, 1993). The incision of the outlet

15 channel complex has lowered the lake level by some 37 m over the last four decades (Watanabe

16 et al., 2009; Lamsal et al., 2011). The outlet flow from the lake forms the river Imja Khola,

17 which is a tributary of the Dudh Koshi river. It is likely that the outlet lake complex is evolving

18 into a new arm of the lake (Benn et al., 2012). The bottom of Imja Tsho is most likely dead ice,

19 given the observed frequency of subaqueous calving and presence of icebergs with apparent

20 subaqueous origins, and the presumed melting of this ice caused the lake level to fall for several

21 decades (Watanabe et al., 1995; Fujita et al., 2009).

22   We conducted a sonar bathymetric survey of Imja Tsho and its outlet complex and a

23 ground penetrating radar (GPR) survey of the Imja-Lhotse Shar glacier in September 2012. The

24 purpose of this paper is to report on the results of those surveys and examine the changes in Imja

25 Tsho volume and area. We rely on a combination of data collected in the field and remotely

26 sensed data to make our analysis.

27

2 Method

2.1 Lake Area Calculation

Bathymetric surveys of Imja Tsho were conducted in April 1992 (Yamada and Sharma, 1993), April 2002 (Sakai et al., 2003), and September 2012 (this study). Landsat satellite imagery is used to compare the areal expansion of Imja Tsho with the changes in bathymetry. Unfortunately, Landsat images from the exact dates of the bathymetric surveys are not available, so the images selected are as close to the survey dates as possible. The images comprise a Landsat-4 image from 4 July 1992 and Landsat-7 images from 4 October 2002 and 29 September 2012. The processing level of the Landsat images are all L1T, indicating that the images are all geometrically rectified using ground control points from the 2005 Global Land Survey in conjunction with the 90 m global DEM generated by the Shuttle Radar Topographic Mission (SRTM). The swipe visualization tool in PCI Geomatica 2013 was used with Landsat band 7 from each image to confirm that the images were properly co-registered. The co-registered images were used to compute changes in the areal extent of Imja Tsho.

The normalized differential water index (NDWI) (McFeeters, 1996) was used to semi-automatically compute the area of the lake. Bolch et al. (2008) found the area of Imja Tsho derived using the NDWI agreed well with a manual delineation performed by Bajracharya et al. (2007), thereby validating the use of the NDWI method. The NDWI was computed using Landsat bands 4 and 5. A threshold of zero was used to classify a pixel as water versus land. Large debris-covered icebergs near the calving front may cause pixels to be misclassified as land rather than water. These pixels are manually corrected in post-processing. Furthermore, at the calving front it can be difficult to distinguish the lake and icebergs from melt ponds located immediately behind the calving front. To prevent misclassification of the calving front, pixels classified as water that are not cardinally connected to the lake are classified as melt ponds. The perimeter of the lake, which is used to quantify uncertainty, is defined as any water pixel that has a land pixel in any cardinal or diagonal direction. The Landsat images have an image-to-image registration accuracy of 7.3 m. The absolute geodetic accuracy is estimated to be ~80 m. When using NDWI we have a maximum error of ±15 m for each pixel.

2.2 Bathymetric Survey

Previous bathymetric surveys of Imja Tsho were conducted in 1992 (Yamada and Sharma, 1993) and 2002 (Sakai et al., 2003; Fujita et al., 2009). In 1992, measurements were taken at 61 points around the lake through holes drilled in the ice using a weighted line. In 2002, measurements were made at 80 uniformly spaced points on the lake using a weighted line. We conducted a bathymetric survey of Imja Tsho between September 22 and 24, 2012 using a Biosonic Habitat EchoSounder MX sonar unit mounted on an inflatable raft. The BioSonics MX Ecosounder (BioSonics, 2012) unit has an accuracy of 1.7cm +/- 0.2% of depth accuracy, 0-100m depth range, single frequency (204.8 kHz) transducer with 8.5 degree conical beam angle, and integrated DGPS with < 3m positional accuracy (Garmin, 2009). Several transects were made around the lake with the sonar unit measuring the depth (Figure 2).

For areas with depths greater than 100 m the equipment does not measure the depth but it still records the position of those points. To estimate the depth of the lake in these areas, we interpolate from the values of the shallower points. To achieve this, transects are established crossing the lake from north to south over these deep areas. The shape of the lake bottom along the transect from north to south is assumed to follow a parabolic shape fit to the measured points which are used to estimate the depths at the missing points.

During the survey, large icebergs blocked access to the eastern end of the lake. Robertson et al. (2012) found that ice ramps at the glacier end of glacial lakes tend to have slopes between 11 and 30 degrees and exhibit subaqueous calving. The level of knowledge of ice ramps in glacial lakes is limited, so it is difficult to determine ramp gradients exactly without detailed bathymetric information. Rather than using the slopes from Robertson et al. (2012), that are more applicable to the Tasman glacier area, the slopes have been changed to resemble the slopes measured at Imja Tsho in 1992 and 2002 by Sakai et al. (2005). Figure 3 shows a longitudinal dashed line in lake following the 1992 and 2002 transect from the western shoreline of the lake to the eastern shoreline reported by Sakai et al. (2005). They found lake bottom slopes near the eastern shoreline in 1992 to be 39 degrees in the first 100 m from the glacier and 12 degrees in the next 200 m; in 2002 the slopes were found to be 32 degrees in the first 50 m, 20 degrees in the next 150 m and 12 degrees in the next 200 m (Sakai et al., 2005, Fig. 6, p. 77). In order to introduce this sloped behavior into the estimation of the lake bottom in the iceberg obstructed

1   area of 2012 and to take account of the uncertainty in the bottom slope, minimum and maximum

2   slopes of the lake floor in front of the glacier terminus were used to approximate bounds for the

3   lake volume in 2012. The maximum slopes were 40 degrees for the first 100 meters from the

4   shoreline, 20 degrees for the next 150 meters, and 5 degrees for the last 150 meters, while the

5   minimum slopes were 20 degrees, 10 degrees, and 2 degrees, respectively. The slopes found by

6   Sakai et al. (2005) are within these bounds.

7   The uncertainty of the lake volume calculation is estimated using a range of depth for

8   each point. In the areas where we were able to measure the depth of the lake we could directly

9   calculate the maximum and minimum values using the error of sonar equipment (1.7 cm $\pm$

10   0.2%*depth). The sonar instrument error applies to every point in the bathymetric survey. In the

11   areas deeper than 100 m, out of the sonar instrument range, the error is higher due to the

12   interpolation calculations, and this error must be added to the instrument error. Quadratic

13   interpolating functions were fit to the points of the 4 transects that have missing data (Figure 2);

14   for points deeper than 100 m, interpolated values and 95% prediction bounds were calculated.

15   The bounds were used to estimate maximum and minimum values associated with each

16   interpolated value. Interpolated values less than 100 m were omitted, since the sonar instrument

17   measured the depth at these points. This results in a cloud of points that cover the measured part

18   of the lake and each point has an associated maximum and minimum value. The points were

19   interpolated to generate 5 m resolution maximum and minimum depth raster files, thus providing

20   two values for each 25 m^2. We assume that the depth in each cell follows a uniform probability

21   distribution (USACE, 2003), which means that all the points within that range, maximum and

22   minimum depth included, have the same probability of being the actual depth of the cell. In

23   order to calculate the volume of the lake we used a Monte Carlo simulation with 2000 samples,

24   which allows us to include the uncertainty in our measurement and assumptions; and calculate

25   the expected value and standard deviation of the water volume.

26   Finally, we have the uncertainty associated with the lake area calculation. The area

27   calculation is performed using the NDWI procedure described in another section. The

28   probability that the NDWI procedure will pick a pixel in the vicinity of the shoreline as lake or

29   land is unknown, so we use a method similar to that just described for the lake volume to include

30   the area calculation error. To estimate the maximum error in the lake area we consider that the

31   lake outline could follow three different lines: the predicted lake outline, and outlines

1 representing the maximum and minimum possible area. The lake volume is calculated for the

2 three lake outlines using the procedure described before.

3

2.3 Ground Penetrating Radar Survey

5 In order to better understand the structure of Imja-Lhotse Shar glacier in the proximity of

6 the eastern end of Imja Tsho, a Ground Penetrating Radar (GPR) survey was conducted and the

7 transect of the survey is shown in (Figure 2). The GPR survey was carried out on 25 September

8 2012 using a custom built, low-frequency, short-pulse, ground-based radar system. Gades et al.

9 (2000) used a similar system on the debris-covered Khumbu glacier near Imja Tsho, but it was

10 not configured for moving transects. The GPR transmitter was a Kentech Instruments Ltd. GPR

11 pulser outputting 4kV signals with a 12V power source. The receiving antenna is connected to

12 an amplifier and a National Instruments USB-5133 digitizer whose output feeds into a LabView

13 program for immediate processing in the field and correlation with GPS signals. Using a

14 common offset, in-line deployment, the GPR pulses are transmitted and received through 10

15 MHz weighted dipole antennae threaded inside climbing webbing. Post-processing steps

16 performed on the data were: topographic correction; pre-trigger points removed; deglitch;

17 demean with smoothing of mean trace; detrend; bandpass filter; convert two-way travel time to

18 depth using a radar velocity in ice of 167×10^6 m/s; depth strip; and normalize by maximum

19 absolute value.

20

3   Results

3.1 Areal Expansion of Imja Tsho

23 The NDWI classifications of water pixels for the Landsat images are shown in white in

24 Figure 4. All the images have pixels identified as melt ponds and the 2012 image has debris-

25 covered icebergs in the lake area both of which are manually corrected for in post-processing.

26 The derived lake areas for the 1992, 2002, and 2012 images are shown in Table 1. The 1992

27 lake area of 0.648 km^2 agrees very well with the 0.60 km^2 lake area measured by Yamada and

28 Sharma (1993) measured in April 1992. The difference between these two measurements may

29 be due to the lake expansion during the 1992 melt season and/or the error associated with the

30 satellite image. The 2002 lake area of 0.867 km^2 also agrees well with the 0.86 km^2 area that

31 Sakai et al. (2003) derived, although the satellite imagery methods used in the referenced study

1   were not described. The good agreement between the derived area and the previous studies

2   demonstrates the effectiveness of using NDWI to outline the lake. The maximum error

3   associated with these area measurements is the number of perimeter pixels multiplied by half the

4   area of a pixel, since pixels on the perimeter that are more than half land would be classified as

5   land. The maximum errors for the three images are also shown in Table 1. The areas of Imja

6   Tsho over the last 50 years are listed in Table 3. We witnessed extensive calving of the eastern

7   glacier terminus, estimated at more than 200 m of ice loss, between May and September of 2012,

8   as indicated in Figure 4 (bottom).

9

10   **3.2 Bathymetric Survey**

11   A contour map of the depth of the Bottom of Imja Tsho derived from the sonar

12   measurements is shown in (Figure 3). Water depths of 20-60 m were measured near the western

13   edge of the lake (outlet end) and 30-100+ m deep near the eastern (glacier) end of the lake.

14   Thick iceberg coverage on the eastern end of the lake prevented transects from being performed

15   up to the calving front. Areas deeper than 100 m were interpolated from the surrounding values

16   as described below. Apparently, the lake bottom has continued to lower as the ice beneath the

17   lake has melted.

18   The bathymetric survey results are reported in Table 2, and they show that Imja Tsho has

19   grown considerably over the last two decades. For example, the maximum depth measured in

20   2002 was 90.5 m (Sakai et al., 2007), compared with a depth of 116.3±5.2 m in the 2012 survey.

21   As a result of the lake expansion and deepening, the estimated volume of water in the lake nearly

22   doubles from the 2002 estimate, i.e., from 35.8±0.7 million m^3 in 2002 to 61.7±3.7 million m^3 in

23   2012. In calculating the uncertainty associated with this volume, we considered the error in the

24   depth measurements, and in the slope of the ice ramp, but not in the lake area. Using the lake

25   area uncertainty calculation method described above, the differences in the volume calculation

26   results using the expected, maximum and minimum lake outlines are on the order of one-half a

27   standard deviation; therefore the error associated with the area estimate is considered negligible

28   and it is not included. The accuracy of the 1992 data are unknown; however, Fujita et al. (2009)

29   estimated the uncertainty of the 2002 data to be ±0.7 million m^3 by assuming the depth

30   measurement error to be 0.5 m. The volume of the lake in 2012 was 72 percent larger than in

1   2002, increasing at an average annual rate of 2.58 million m^3 yr^{-1}. Compared to the prior surveys,

2   the results show that the eastern section of the lake has deepened over the last decade (2002-2012)

3   as the ice beneath has melted, with the average depth increasing by 0.86 m yr^{-1}. In the same

4   period, the maximum depth has increased 28.5%, or an annual rate of 2.58 m yr^{-1}.

5   Figure 5 shows the 2012 bathymetric survey results along section A-A' from Figure 3

6   along with those of the 2002 survey (Sakai et al., 2003, Fig. 4, p. 559), indicating an eastward

7   expansion of the lake, rapid retreat of the glacier ice cliff and the subaqueous melting that has

8   taken place. The data from the 2002 survey (location and depth) were provided to us by the

9   authors (K. Fujita pers. communication 14 July 2014) and can be depicted in Figure 5 by

10   assuming that the lake surface has not changed since 2002. This assumption is reasonable as

11   various studies have shown that the level of the lake has not changed significantly since 2002

12   (Sakai et al., 2007; Lamsal et al., 2011; Fujita et al., 2009).

13   Two distinct zones of Imja Tsho with different depths are illustrated in Figure 5: zone A,

14   from 0 m to 1,000 m on (western part), and zone B, from 1,000 m to 2,100 m (eastern part). The

15   exact separation between these two zones is unknown, but it is estimated from the bathymetric

16   data to occur at about 1,000 m on Figure 5. Reasons for the differences in depth between the two

17   zones are not entirely clear, but may be related to the presence or non-presence of ice at the lake

18   bottom. That is, a lack of dead ice at the bottom of zone A would arrest all further deepening,

19   while the presence of ice at the bottom of zone B would account for its continued deepening.

20   This might also be due to a thick debris cover on the ice at the bottom of zone A. When the lake

21   grew to form the western part (zone A), the growth rate was much smaller; therefore, more

22   debris might have deposited on the lake bottom. Later, when zone B was formed, the rapid

23   growth may not have resulted in thick debris to form on the lake bottom.

24

25   **3.3 Retreat of Imja-Lhotse Shar Glacier**

26   The areal expansion of Imja Tsho is primarily in the eastward (up-glacier) direction due

27   to the retreat of the calving front. The calving front was defined in the NDWI image processing

28   as the last pixel in each row that has a lake pixel to its left and a land pixel to its right. A

29   problem arises in the southern-most calving front pixels in which a calving front pixel is defined

30   in a later image, but is not defined in an earlier image because the lake's width expanded. In this

1 circumstance, which occurs three times between the 1992 and 2002 images and two times

2 between the 2002 and 2012 images, the calving front pixel for the older image is considered

3 equal to the closest calving front pixel. The expansion rate for a row may then be computed as

4 the difference between calving front pixels within a given row. The maximum error in this

5 expansion rate estimate is one pixel. The average retreat distances for 1992-2002, 2002-12, and

6 1992-2012 are shown in Table 4. From 2002 to 2012 the retreat greatly increased to 526m (52.6

7 m yr^{-1}). The corresponding standard deviations are large due to the calving front having an arm-

8 like shape in 2002, which caused a non-uniform rate of retreat. The overall expansion rate from

9 1992 to 2012 was 43.0 m yr^{-1}.

10

11 **3.4   Drainable Water from Imja Tsho**

12 Using the data reported above, we calculated the volume of water that could possibly

13 drain from the lake for various levels of the lake surface. In the event of a breach of the former

14 glacier terminus, water may not drain from the lake all at once and the timing or the hydrograph

15 of the drainage is important in order to estimate the critical water volume that might cause

16 serious damage downstream. However, detailed calculation of the volume and timing of

17 discharge in the event of a breach of Imja Tsho requires extensive numerical simulations and is

18 beyond the scope of this paper. Due to the continued areal expansion of the lake, there is an

19 increasing amount of water that could drain from the lake in the event of a breach; however, this

20 does not necessarily mean that there is an increases probability of occurrence of such an event.

21 Figure 6 shows the resulting drainage volume for various lake elevations. The maximum

22 amount of water that could be released from the lake is 34.1±1.08 million m^3, if the lake surface

23 elevation decreases from 5010 m to 4975 m (the elevation of the valley floor below the lake). In

24 a previous (2002) estimate, this volume was 20.6 million m^3 (Sakai et al., 2007). The 2012

25 estimate is 40.5% larger than the 2002 value. This level of potential drainage water is a rough

26 estimate and would require a complete collapse of damming moraine, which may be unlikely

27 since Imja Tsho is dammed by a wide moraine (> 500 m). Fujita et al. (2013) note that for

28 Himalayan glacial lakes, if the damming moraine is wide enough or the height difference

29 between the lake surface and the downstream valley is small enough, such a lake is unlikely to

30 cause a GLOF. The relative height between lake surface and the base of moraine is not precisely

1   known by land survey techniques. However, others have discussed the topography around the

2   lake. The lake surface has lowered gradually over the past three decades (Lamsal et al., 2011) to

3   a stable level of 5009 – 5010 m and the lake surface elevation is generally acknowledged to have

4   been stable at about 5010 m for over a decade (Fujita et al., 2009; Lamsal et al., 2011).

5   Fujita et al. (2013) proposed an index method for characterizing Potential Flood Volume

6   (*PFV*) from glacial lakes in the Himalaya. The method is based on the depression angle between

7   the lake water surface and any point within 1 km downstream. The potential lowering height (H_p,

8   m) is the level that the lake must be lowered to so that the depression angle will be 10 degrees.

9   *PFV* is defined as

10         $PFV = \text{minimum}[H_p; D_m]*A$ (1)

11   where H_p is the potential lowering height, D_m is the mean depth (m) and A is the area (km^2) of

12   the lake, respectively. One of the difficulties in applying this method at Imja Tsho is defining the

13   point at the lake from which to start the calculation. We considered three starting points for the

14   *PFV* calculations: the western end of the main lake; midway from the main lake to the end of the

15   outlet; and the end of the outlet (Table 5). We assumed the elevation of the lake and outlet are

16   5010 m and the downstream point is located where the outlet stream enters the valley below the

17   moraine at 4975 m. If the starting location is at the end of the lake outlet, then PFV = 11.3

18   million m^3, but starting from the other locations results in a *PFV* = 0. Certainly, the first case is a

19   maximum one and can only occur is there is a complete collapse of the moraine. Fujita et al.

20   (2013) imply that lowering the lake level to the point where the depression angle is less than 10

21   degrees may reduce this risk, which would require lowering the lake 9 m and removing of 11.3

22   million m^3 of water from the lake. This would represent a minimum level of lake lowering, since

23   the PFV does not consider the condition of the moraine or possible breach triggering

24   mechanisms. It is possible that the end of outlet complex should not be used in the calculations

25   because it does not properly take into account the width of the moraine. Fujita et al. (2013)

26   calculated a PFV of zero for Imja Tsho (because Hp = 0 < Dm), indicating that it that is

27   reasonably safe at that time. They note that future lowering of the moraine dam may possibly

28   result in future changes to the lakeshore downstream (Fujita et al., 2009); therefore, continuous

29   monitoring of such large-scale lakes is required. Thus, understanding the bathymetry of these

30   large glacial lakes is very important.

1

3.5 GPR Survey of Imja-Lhotse Shar Glacier

3   Figure 7 shows the results of the GPR survey for the transect across the Imja-Lhotse Shar

4   glacier from north to south using a 10Mhz antenna and assuming a velocity of propogation

5   through the ice of 167×10^6 m/s. The thickness of the glacier varies from 40-60 m near the lateral

6   moraines to over 200 m in the center of the glacier. The implications of the glacier thickness and

7   present lake depth are discussed below.

8

3.6 Conceptual Model of Imja Tsho

10   Figure 8 shows a vertical cross-section of a conceptual model of Imja Tsho created from

11   the bathymetric and GPR survey data as well as a 5 m resolution digital elevation model (Lamsal

12   et al., 2011) for the topography of the up-glacier area on the eastern end of the lake and the

13   outside face of the moraine on the western end of the lake. The bottom of the Imja-Lhotse Shar

14   glacier near the glacier terminus was determined from the GPR survey. The exact boundaries of

15   the debris and ice areas and the lower bedrock and the glacier ice are unknown and shown as

16   such in the figure using question marks (?). Similarly, the depth of mixed debris and ice in the

17   western moraine end of the lake are mostly unknown. There is great difficulty in defining the

18   boundary between the area of the lake underlain by ice as opposed to ice and rock or just rock.

19

4   Conclusions

21   The results of a 2012 bathymetric survey of Imja Tsho show that the lake has deepened

22   from 98 m in 2002 to 116.3±5.2 m in 2012. Likewise, the volume has increased from 35.8±0.7

23   million m^3 to 61.7±3.7 million m^3 over the past decade as well, a 70 percent increase. The lake

24   volume is increasing at a rate of 2.51 million m^3 yr^{-1}, and the average depth is increasing by 0.86

25   m yr^{-1}. Our survey results also suggest that the lake bottom has continued to lower as the ice

26   beneath it has melted. Most of the expansion of the lake in recent years has been due to the

27   retreat of the glacier terminus (eastern end of the lake) through calving processes. The rate of

28   retreat of the glacier terminus, indicating the growth of the lake, has increased to 52.1 m yr^{-1} over

29   the last decade and the areal expansion rate has increased to 0.038 km^2 yr^{-1}. The results of the

30   GPR survey for the transect across the Imja-Lhotse Shar glacier show that the ice-bedrock

interface is significantly below the lake bottom with an ice thickness over 200 m in the center of the glacier. The continued expansion of the lake has increased the maximum volume of water that could be drained from the lake in the event of a breach in the damming moraine to 34.1 ± 1.08 million m^3, rather than 21 million m^3 estimated in 2002 if the lake surface elevation decreases from 5010 m to 4975 m (the elevation of the valley floor below the lake).

Acknowledgements

References

Bajracharya, S. R., Mool, P. K., Shrestha, B. R.: Impact of Climate Change on Himalayan Glaciers and Glacial Lakes: Case Studies on GLOF and Associated Hazards in Nepal and Bhutan, International Centre for Integrated Mountain Development (ICIMOD), Kathmandu, 2007.

Bajracharya, S. R., Mool, P. K.: Glaciers, glacial lakes and glacial lake outburst floods in the Mount Everest region, Nepal, Annals of Glaciology 50(53):81-86, 2009

Benn, D. I., Bolch, T., Hands, K., Gulley, J., Luckman, A., Nicholson, L. I., Quincey, D., Thompson, S., Toumi, R., Wiseman, S.: Response of debris-covered glaciers in the Mount Everest region to recent warming, and implications for outburst flood hazards, Earth-Science Reviews 114:156–174, 2012.

Biosonics, Inc. MX Series Specifications and Features, Seattle Washington 2012. http://www.biosonicsinc.com/product-mx-habitat-echosounder.asp#specsheet <accessed 16 July 2012>

Bolch, T., Buchroithner, M. F., Peters, J., Baessler, M., Bajracharya, S. R.: Identification of glacier motion and potentially dangerous glacier lakes at Mt. Everest area/Nepal using spaceborne imagery, Natural Hazards and Earth System Sciences 8, 1329-1340, 2008.

Bolch, T., Pieczonka, T., Benn, D. I.: Multi-decadal mass loss of glaciers in the Everest area (Nepal Himalaya) derived from stereo imagery, The Cryosphere, 5, 349–358, 2011.

Byers, A. C.: An assessment of contemporary glacier fluctuations in Nepal's Khumbu Himal using repeat photography, Himalayan Journal of Sciences, 4(6):21-26, 2007.

Carrivick, J. L., Rushmer, E. L.: Understanding high-magnitude outburst floods, Geology Today 22, 60–65, 2006.

Fujita, K., Sakai, A., Nuimura, T., Yamaguchi, S., Sharma, R. R.: Recent changes in Imja Tsho and its damming moraine in the Nepal Himalaya revealed by in-situ surveys and multi-temporal ASTER imagery, Environmental Research Letters 4, 045205 (045207pp), doi:045210.041088/041748-049326/045204/045204/045205, 2009.

Fujita, K., Sakai, A., Takenaka, S., Nuimura, T., Surazakov, A. B., Sawagaki, T., and Yamanokuchi, T.: Potential flood volume of Himalayan glacial lakes, Nat. Hazards Earth Syst. Sci., 13, 1827-1839, 2013.

Gardelle, J., Arnauda, Y., Berthier, E.: Contrasted evolution of glacial lakes along the Hindu Kush Himalaya mountain range between 1990 and 2009, Global & Planetary Change 75(1-2):47-55, 2011.

Gardelle, J., Berthier, E., Arnaud, Y., Kääb, A.: Region-wide glacier mass balances over the Pamir-Karakoram-Himalaya during 1999–2011, The Cryosphere, 7, 1263–1286, 2013, doi:10.5194/tc-7-1263-2013.

Garmin (2009), GPS 15xH/15xL Technical Specifications, 190-00266-03 Rev. A, Garmin International, Inc. Olathe, Kansas USA December, 2009.

Hagen, T., Dyrenfurth, G. O., von Fürer-Haimendorf, C., Schneider, E. (eds.): Mount Everest: Formation, Population and Exploration of the Everest Region. Oxford University Press, London, 1963.

Hambrey, M. J., Quincey, D. J., Glasser, N. F., Reynolds, J. M., Richardson, S. J., Clemmens, S.: Sedimentological, geomorphological and dynamic context of debris-mantled glaciers, Mountain Everest (Sagarmatha) region, Nepal. Quaternary Science Reviews 27: 2361–2389, 2008.

Hammond, J. E.: Glacial lakes in the Khumbu region, Nepal: An assessment of the hazards. Unpublished MA Thesis, University of Colorado, Boulder, CO, 1988.

Ives, J. D., Shrestha, R. B., Mool, P. K.: Formation of glacial lakes in the Hindu Kush-Himalayas and GLOF risk assessment, International Centre for Integrated Mountain Development (ICIMOD), Kathmandu, 2010.

Jianchu, X., Shrestha, A., Vaidya, R., Eriksson, M., Hewitt, K.: The Melting Himalayas: Regional Challenges and Local Impacts of Climate Change on Mountain Ecosystems and Livelihoods, ICIMOD Technical Paper, International Centre for Integrated Mountain Development (ICIMOD) Kathmandu, 2007.

Lamsal, D., Sawagaki, T., Watanabe, T.: Digital Terrain Modelling Using Corona and ALOS PRISM Data to Investigate the Distal Part of Imja-Lhotse Shar glacier, Khumbu Himal, Nepal. J. Mt. Sci. 8: 390-402, 2011.

McFeeters, S.: The use of the normalized difference water index (NDWI) in the delineation of open water features, International Journal of Remote Sensing, 17(7), 1425–1432, 1996.

Mool, P. K., Bajracharya, S. R., Joshi, S. P.: Inventory of Glaciers, Glacial Lakes and Glacial Lake Outburst Floods: Monitoring and Early Warning Systems in the Hindu Kush-Himalayan Region, Nepal, International Centre for Integrated Mountain Development (ICIMOD), Kathmandu, 2001.

Nuimura, T., Fujita, K., Yamaguchi, S., Sharma, R. R.: Elevation changes of glaciers revealed by multitemporal digital elevation models calibrated by GPS survey in the Khumbu region, Nepal Himalaya, 1992–2008, Journal of Glaciology, Vol. 58, No. 210, 2012.

Quincey, D. J., Richardson, S. D., Luckman, A., Lucas, R. M., Reynolds, J. M., Hambrey, M. J., Glasser, N. F.: Early recognition of glacial lake hazards in the Himalaya using remote sensing datasets, Global and Planetary Change 56 (2007) 137–152, 2007.

Robertson, C. M., Benn, D. I., Brook, M. S., Fuller, I. C., Holt, K. A.: Subaqueous calving margin morphology at Mueller, Hooker and Tasman glaciers in Aoraki/Mount Cook National

Park, New Zealand, Journal of Glaciology, Vol. 58, No. 212, 2012.

Sakai, A., Fujita, K., Yamada, T.: Volume change of Imja Tsho in the Nepal Himalayas, Disaster Mitigation and Water Management, December 7-10 ISDB 2003, Niigate, Japan, 2003.

Sakai, A., Fujita, K., Yamada, T.: Expansion of the Imja glacier Lake in the East Nepal Himalaya. In: Mavlyudov, B.R. (Ed.), Glacier Caves and Glacial Karst in High Mountains and Polar Regions: 7th GLACKIPR Symposium. Institute of geography of the Russian Academy of Sciences, Moscow, pp. 74-79, 2005

Sakai, A., Saito, M., Nishimura, K., Yamada, T., Iizuka, Y., Harada, K., Kobayashi, S., Fujita, K., Gurung, C.B.: Topographical survey of end-moraine and dead ice area at the Imja Glacial Lake in 2001 and 2002. Bulletin of Glaciological Research, 24, 29-36, 2007.

Shrestha, A. B., Aryal, R.: Climate change in Nepal and its impact on Himalayan glaciers, Regional Environmental Change, 11 (Suppl 1):S65–S77 doi:10.1007/s10113-010-0174-9, 2011.

UNDP - United Nations Development Programme: Community Based Glacier Lake Outburst and Flood Risk Reduction in Nepal. Project Document, UNDP Environmental Finance Services, Kathmandu, Nepal, 2013.

USACE – United States Army Corps of Engineers: Uncertainty in Bathymetric Surveys, Coastal and Hydraulics Engineering Technical Note ERDC/CHL CHETN-IV-59, 2003.

Watanabe, T., Ives, J. D., Hammond, J. E.: Rapid growth of a glacial lake in Khumbu Himal, Himalaya: prospects for a catastrophic flood, Mountain Research and Development 14(4): 329–340, 1994.

Watanabe, T., Kameyama, S., Sato, T.: Imja-Lhotse Shar glacier dead-ice melt rates and changes in a supra-glacial lake, 1989-1994, Khumbu Himal, Nepal: Danger of lake drainage, Mountain Research and Development 15(4): 293–300, 1995.

Watanabe, T., Lamsal, D., Ives, J. D.: Evaluating the growth characteristics of a glacial lake and its degree of danger of outburst flooding: Imja-Lhotse Shar glacier, Khumbu Himal, Nepal, Norsk Geografisk Tidsskrift 63(4): 255–267, 2009.

Yamada, T.: Glacier lakes and its outburst flood in the Nepal Himalaya, Monograph No.1, Data Centre for Glacier Research, Japanese Society of Snow and Ice, 1998.

1   Yamada, T., Sharma, C. K.: Glacier Lakes and Outburst Floods in the Nepal Himalaya, in Snow

2   and Glacier Hydrology, Proc., Kathmandu Symposium, Nov. IAHS Publication No. 218, 1993.
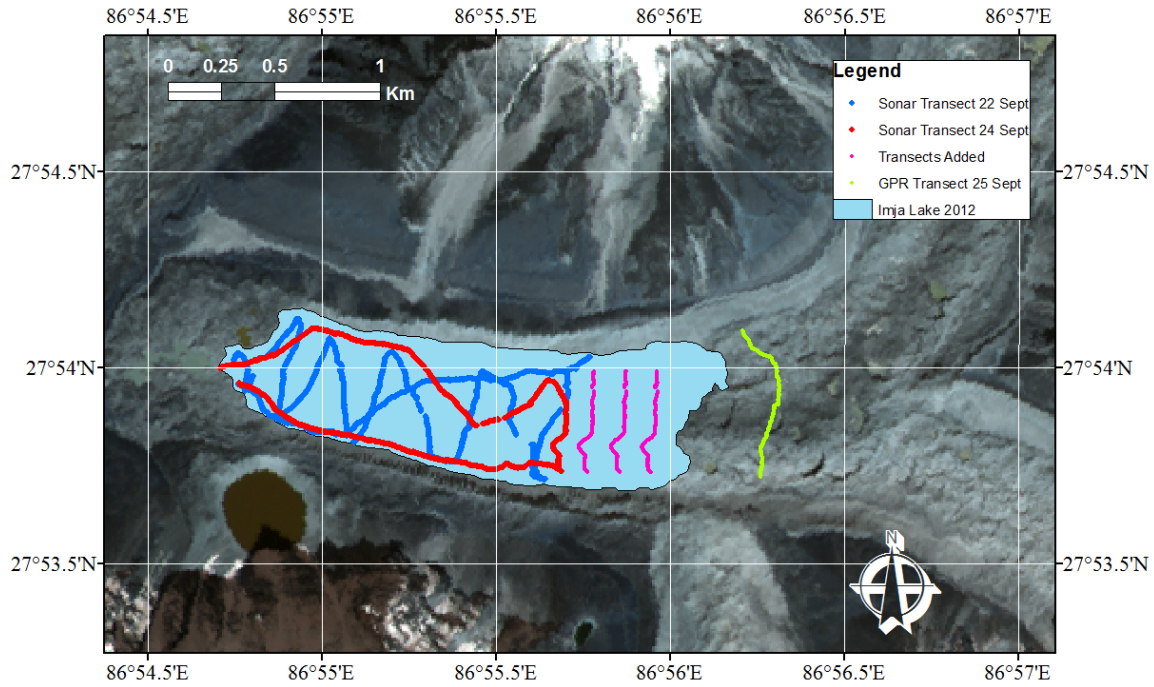
3
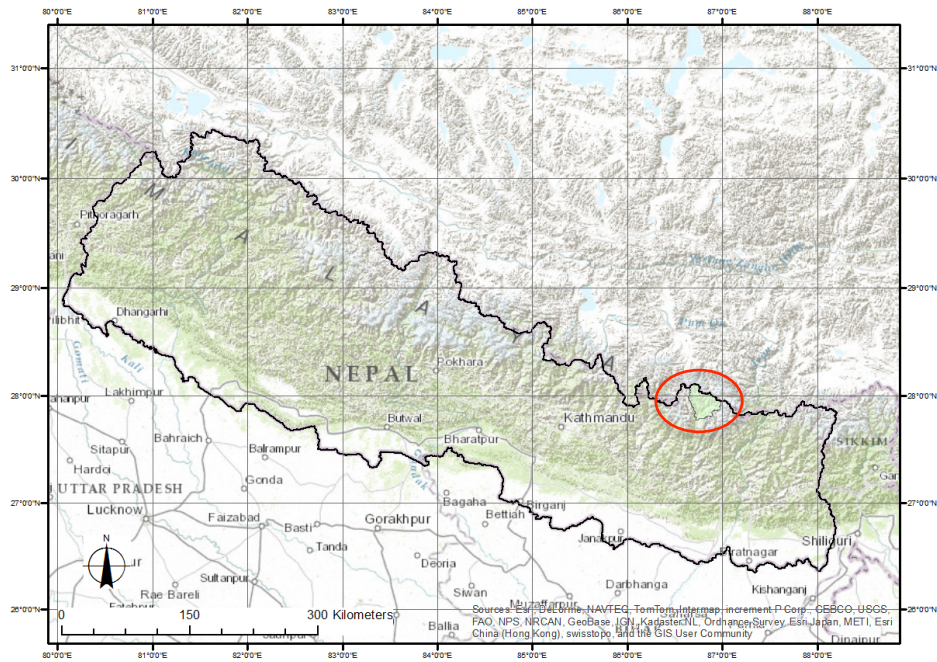
1

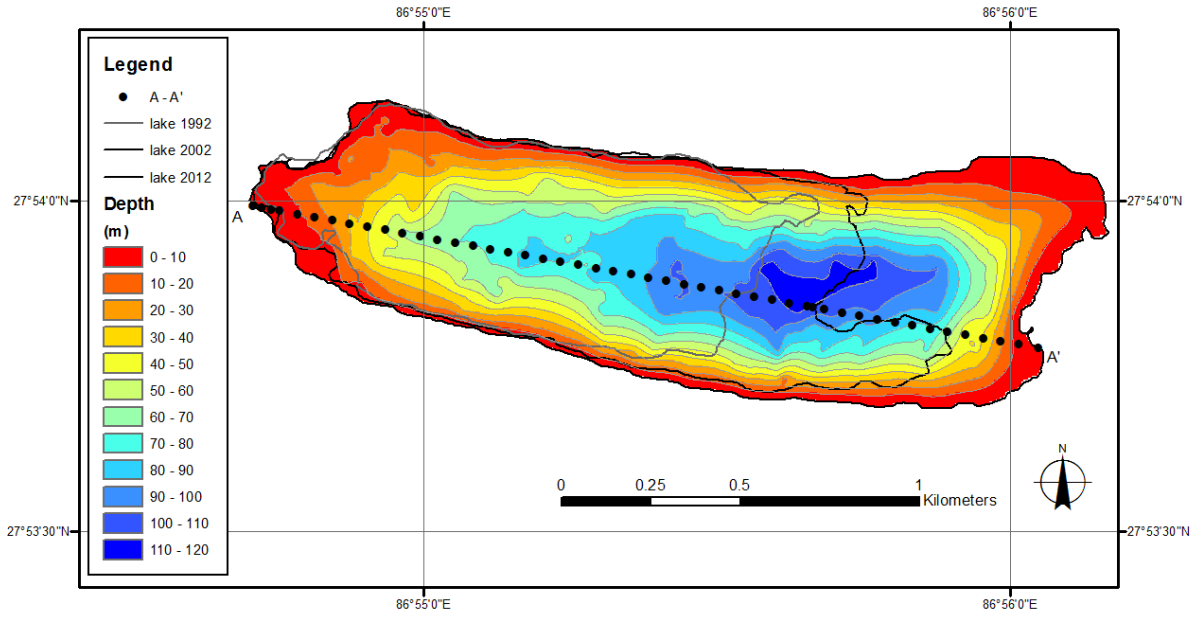2 Figure 1. Location of the Khumbu region of Nepal.

3

1

2

3 Figure 2. Sonar bathymetric survey transects at Imja Tsho September 22 (red) and 24 (blue), the

4 transects used to interpolate missing values (pink), and the GPR transect at Imja-Lhotse Shar

5 glacier September 25 (green). The background is an ALOS image from 2008.
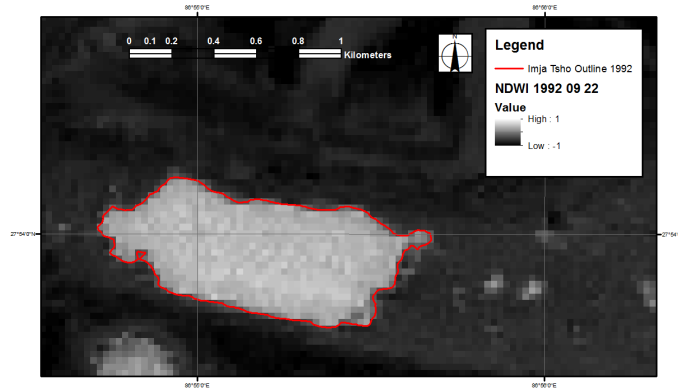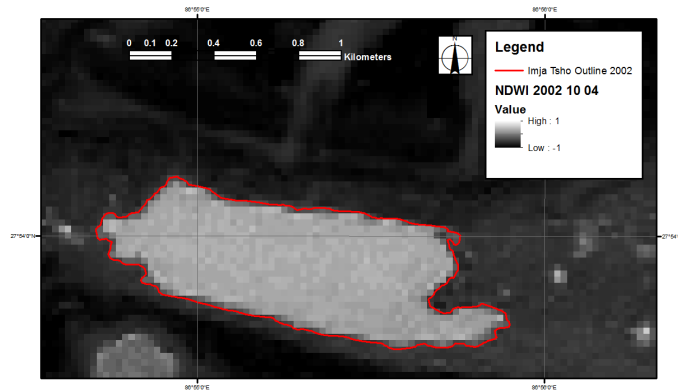
6

19

Figure 3. Bathymetric survey results from Imja Tsho in September 2012.
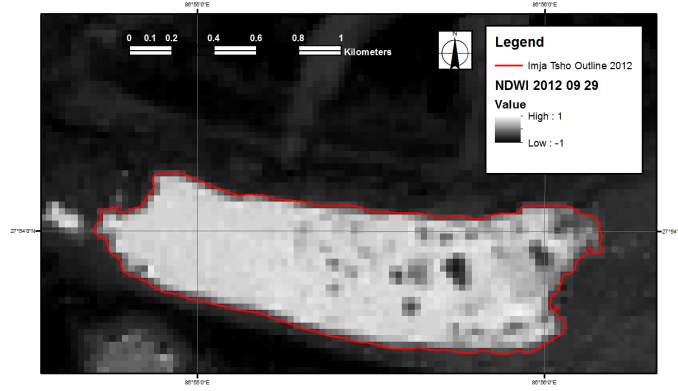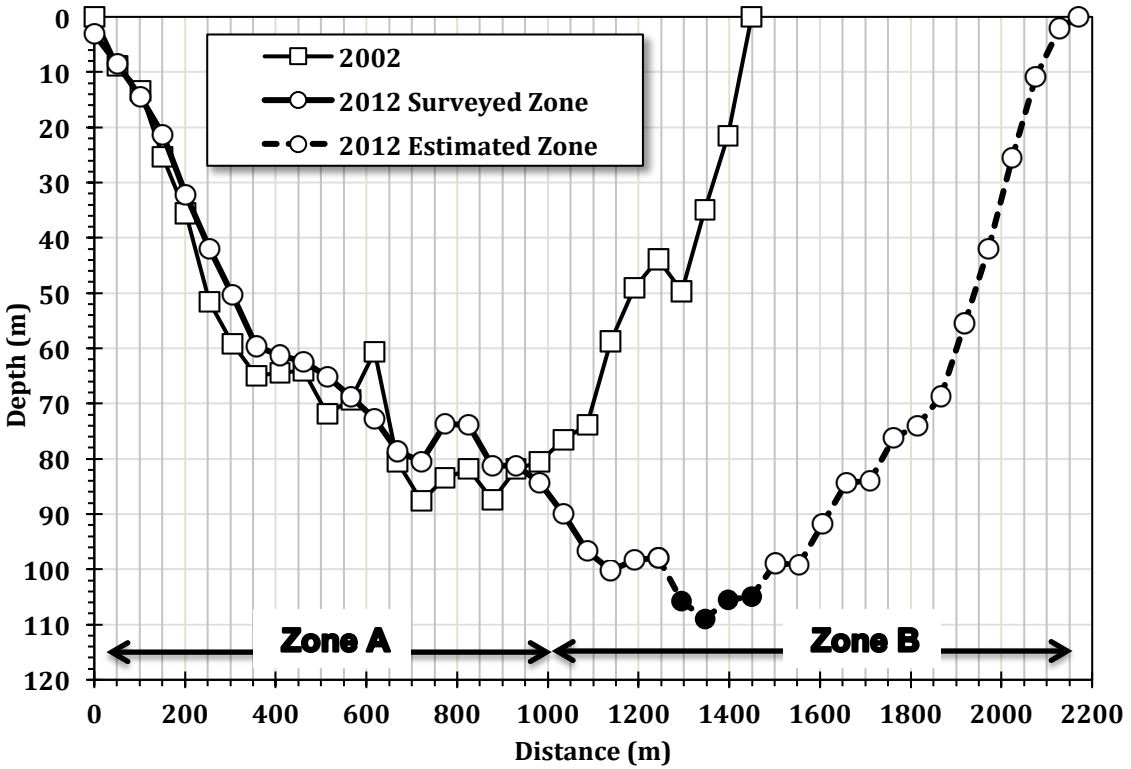
1

2

3

4   Figure 4. NDWI calculated from Landsat images for dates associated with bathymetric surveys

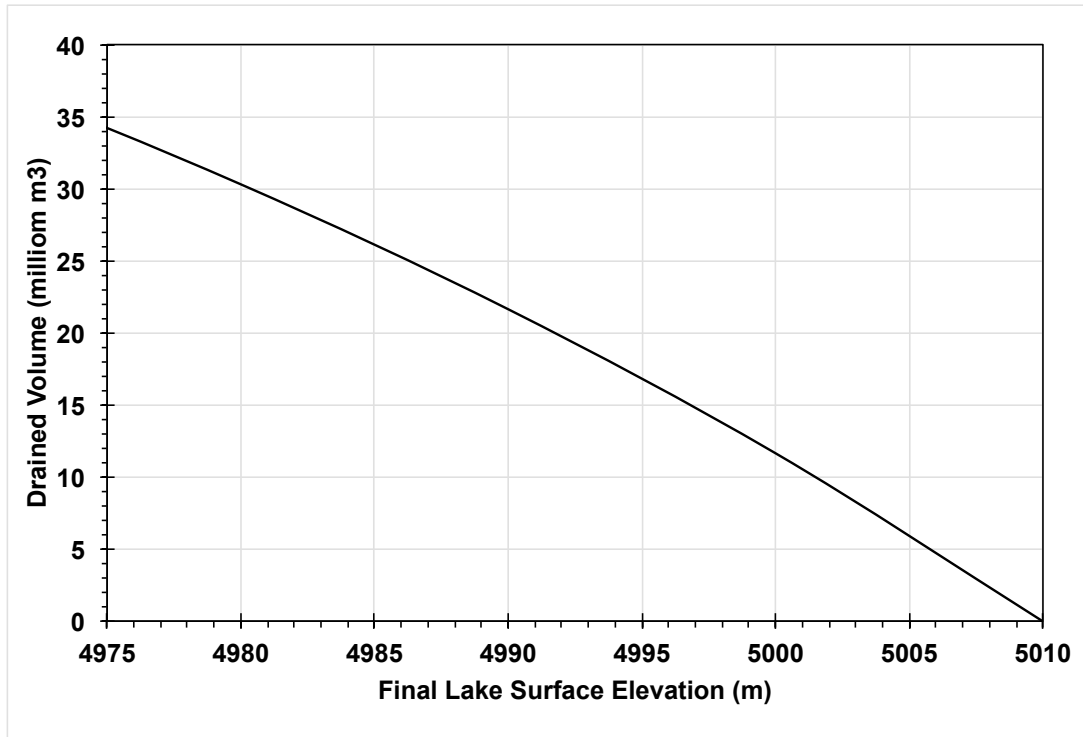5   in 1992 (top), 2002 (middle) and 2012 (bottom).

6

1

Figure 5. Cross-section A-A' of the 2012 bathymetric survey for Imja Tsho compared to the 2002 survey. The solid indicates surveyed points and dashed line indicates estimated points. The filled circle markers indicate points deeper than 100 m where interpolation was used.
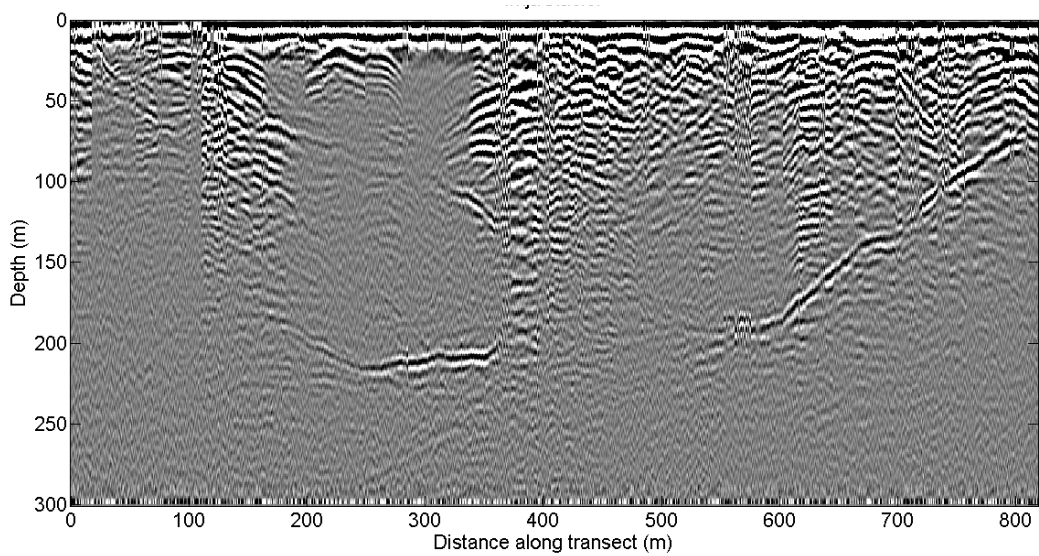
2

3

4

5

6

7

1

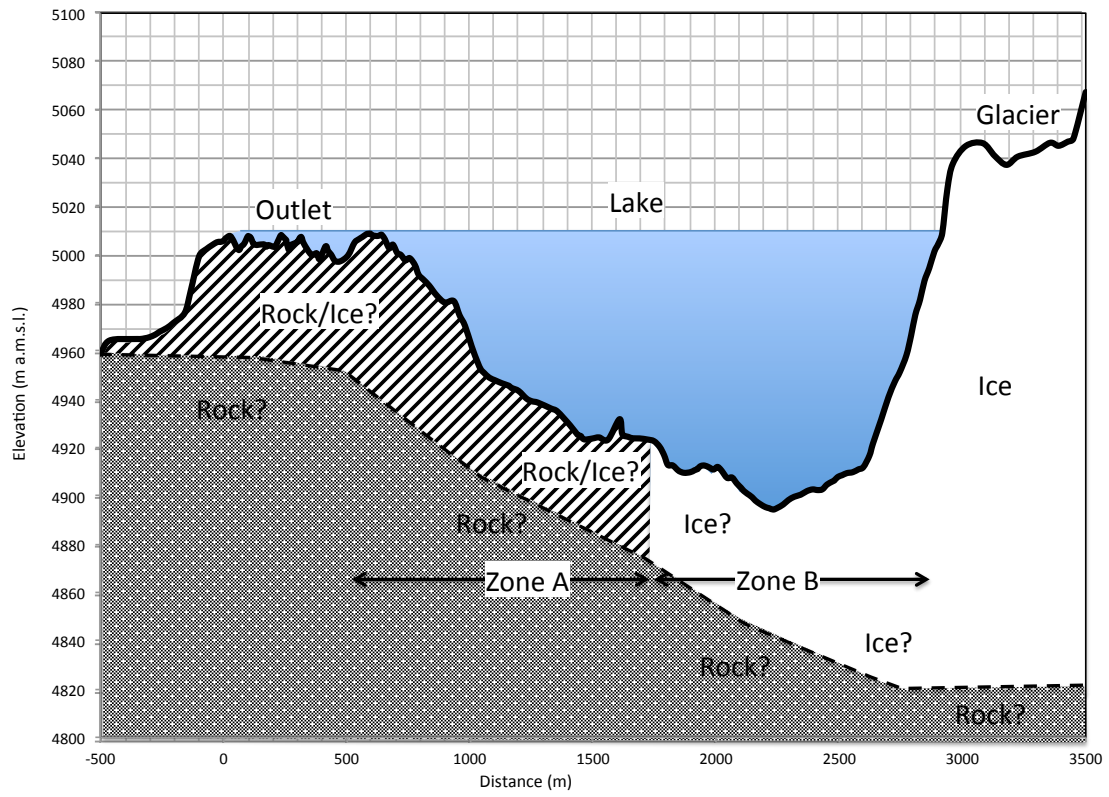2 Figure 6. Potentially drained volume from Imja Tsho versus lake surface elevation.

3

4

5 Figure 7. GPR transect across Imja/Lhotse Shar glacier from North to South on 25 September

6 2012 using a 10 MHz antenna and velocity in ice of 167×10^{6} m/s.

7

Figure 8. Conceptual model of Imja Tsho.

Table 1. Imja Tsho Area Expansion 1992-2012.

Year	Icebergs (no.)	Melt Ponds (no.)	Lake Pixels (no.)	Perimeter Pixels (no.)	Area (km^2)	Max. Error (km^2)	Decade Expansion Rate (km^2 yr^{-1})
1992[1]					0.60		
1992[3]	0	12	720	162	0.648	0.073	
2002[2]					0.868		0.026
2002[3]	0	28	963	202	0.867	0.091	0.022
2012[3]	15	2	1397	231	1.257	0.104	0.039

[1] Yamada and Sharma (1993)

[2] Fujita et al. (2009)

[3] This study

Table 2. Comparison of Imja Tsho 2012 Bathymetric Survey Results with Previous Studies. The 2012 volume and average depth uncertainty are 95% confidence bounds from the Monte Carlo sampling result. Maximum depth uncertainty is calculated from the 95% prediction bounds.

Study	No. of points	Volume (10^6 m^3)	Ave. Depth (m)	Max. Depth (m)
1992 (Yamada and Sharma 1993)	61	28.0	47.0	98.5
2002 (Sakai et al., 2003)	80	35.8±0.7	41.6	90.5
2012 (This study)	10,020	61.7±3.7	48.0±2.9	116.3±5.2

Table 3. Imja Tsho Area Expansion 1962-2012.

Year	Area (km^2)	Uncertainty (km^2)	Reference
1962	0.028		Bajracharya. et al. (2007)
1964	0.068		Lamsal et al. (2011)
1975	0.310		Bajracharya. et al. (2007)
1983	0.569		Bajracharya. et al. (2007)
1989	0.633		Bajracharya. et al. (2007)
1992	0.636		Bajracharya. et al. (2007)
1992	0.648	0.073	This study
2000	0.844	0.036	Fujita et al. (2009)
2000	0.775		Bajracharya. et al. (2007)
2000	0.766		Bolch et al. (2008)
2000	0.838	0.263	Gardelle et al. (2011)
2001	0.827	0.040	Fujita et al. (2009)
2001	0.824		Bajracharya. et al. (2007)
2002	0.868	0.037	Fujita et al. (2009)
2002	0.867	0.091	This Study
2003	0.889	0.039	Fujita et al. (2009)
2004	0.928	0.041	Fujita et al. (2009)
2005	0.896	0.042	Fujita et al. (2009)
2006	0.897	0.041	Fujita et al. (2009)
2006	0.913		Lamsal et al. (2011)
2006	0.941		Bajracharya. et al. (2007)
2007	1.030		Watanabe et al. (2009)
2008	0.920	0.036	Fujita et al. (2009)
2009	1.012		Watanabe et al. (2009)
2009	1.138	0.328	Gardelle et al. (2011)
2012	1.257	0.104	This study

3

1

Table 4. Retreat of Imja-Lhotse Shar Glacier for 1992-2012 Based on Landsat Images.

	Retreat			
Period	Average (m)	Std. Dev. (m)	Max. Error (m)	Expansion Rate (m yr^{-1})
1992-2002	316	201	30	31.6
2002-2012	526	231	30	52.6
1992-2012	861	83	30	43.0

3

Table 5. PFV Calculations for Imja Tsho Considering Three Starting Points on the Lake or Outlet.

	Calculation starting location			
	Lake	Outlet middle	Outlet end	Reduce to 10 deg
Distance (m)	641	364	150	150
Height (m)	35	35	35	26
Depression Angle (degrees)	3.1	5.5	13.5	10.0
A (km^2)				1.257
Hp (m)				9
PFV (million m^3)				11.3

6